SAND2024-06524C

Applications of 3D EBSD for understanding complex microstructures

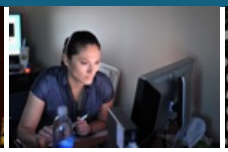

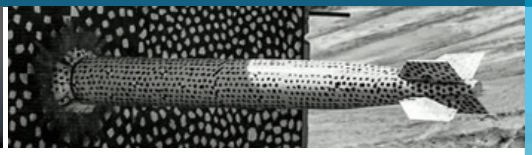

Andrew Polonsky, *Julia Deitz, Hojun Lim, Philip Noel, Michael Melia, Kyle Johnson, Peter Renner, Kasandra Herrera, Luis Jauregui, and Damion Cummings*

Monday, March 4, 2024

Sandia National Laboratories is a multimission laboratory managed and operated by National Technology & Engineering Solutions of Sandia, LLC, a wholly owned subsidiary of Honeywell International Inc., for the U.S. Department of Energy's National Nuclear Security Administration under contract DE-NA0003525.

Outline

- Motivation
- Orientation Gradients in 3D
- Multimodal Data Fusion
- EBSD Distortion Correction
- Integration with Modeling
- Conclusion

3D Characterization has Advanced Significantly in the last Decade

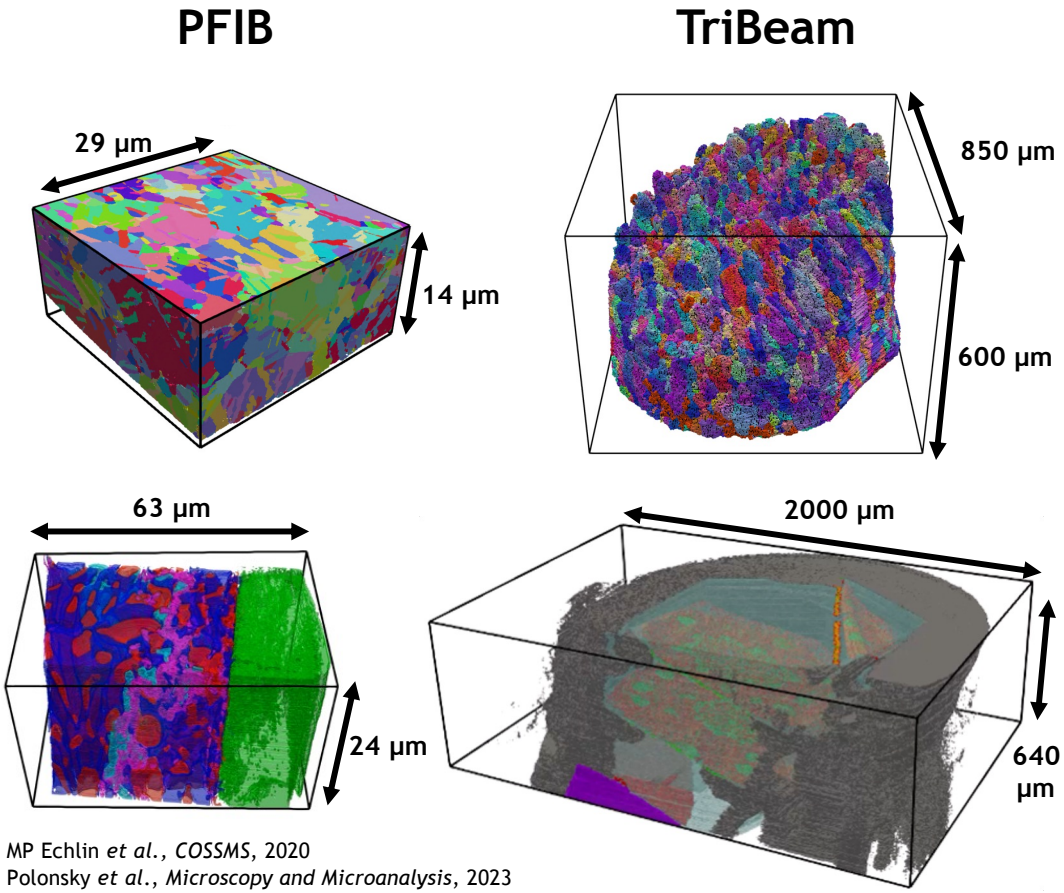

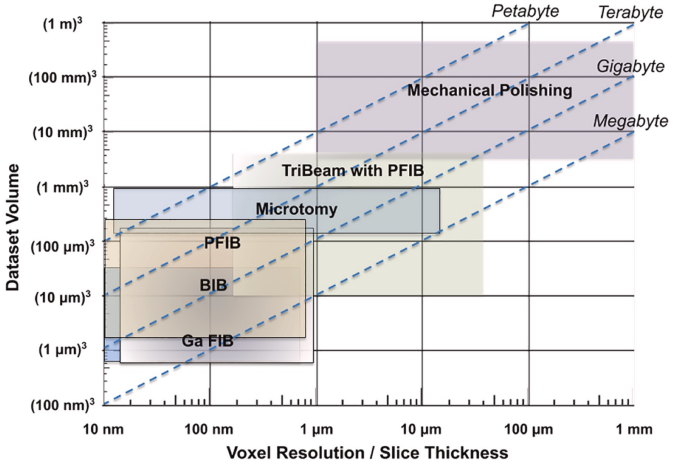

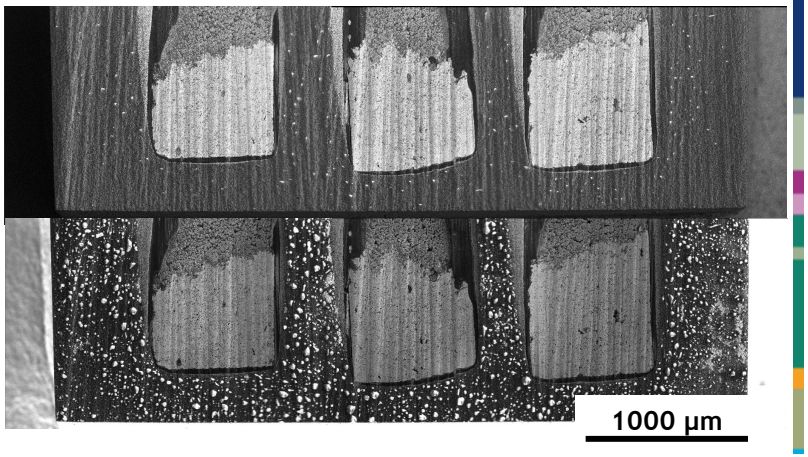

MP Echlin *et al.*, *COSSMS*, 2020
Polonsky *et al.*, *Microscopy and Microanalysis*, 2023

Complex 3D microstructures exhibit large orientation gradients

- Well-annealed or undeformed crystals are easily analyzed with approaches using 2D conventions

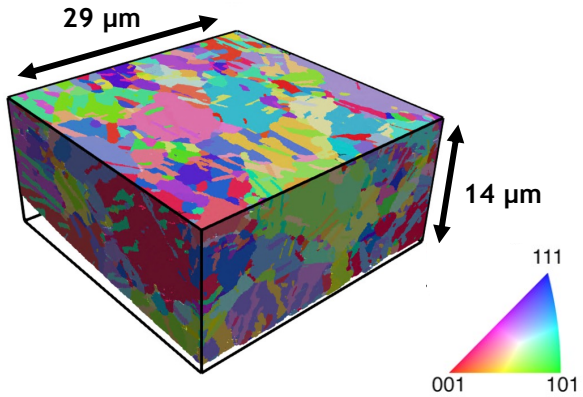

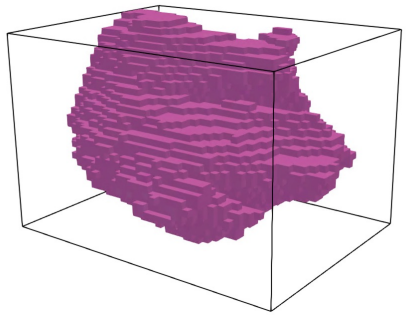

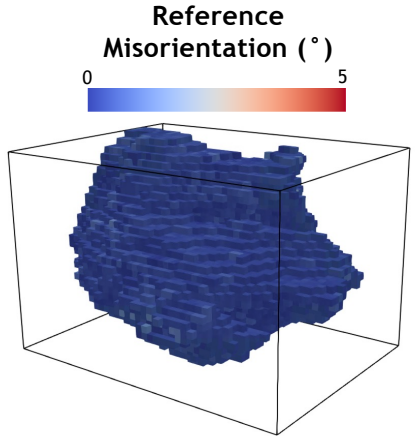

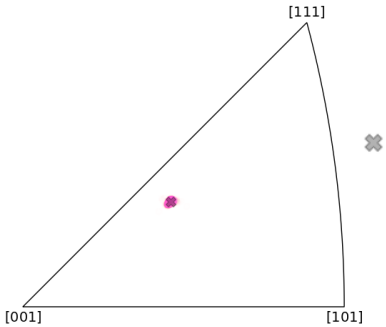

Average Orientation

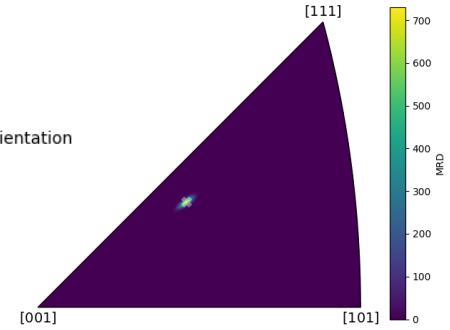

Complex 3D microstructures exhibit large orientation gradients

- Average orientation is not necessarily a good reference in all cases

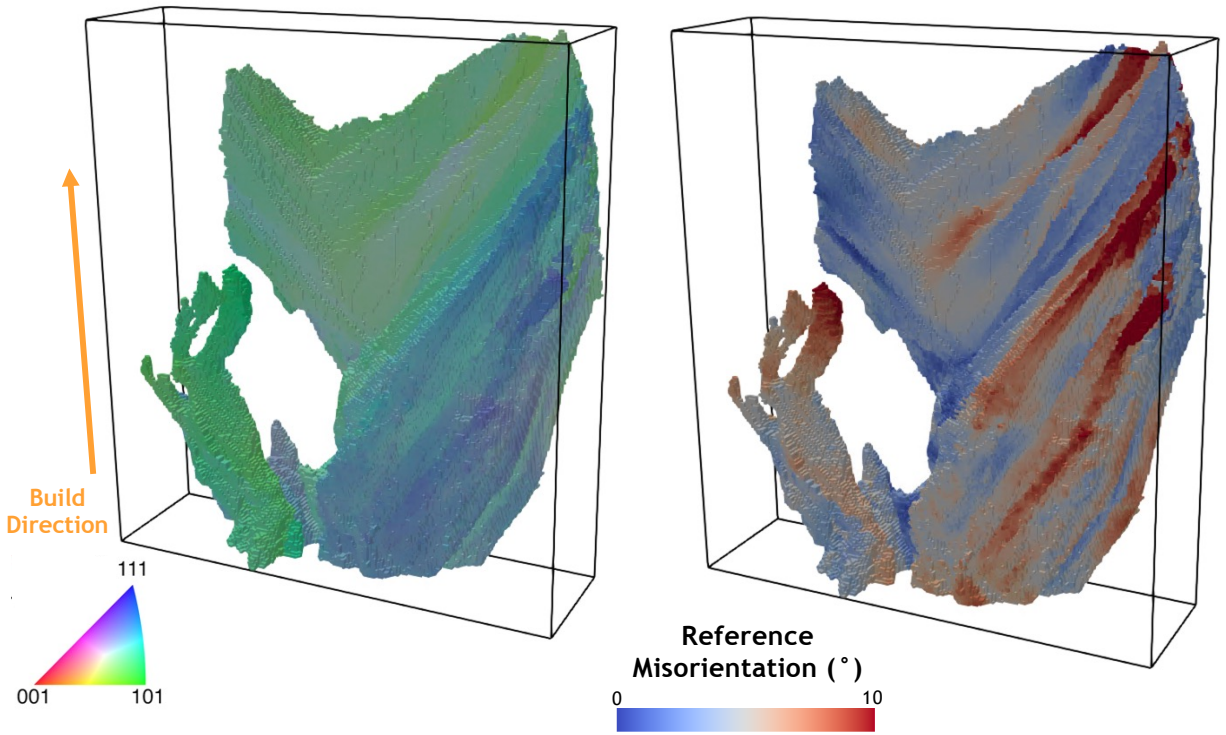

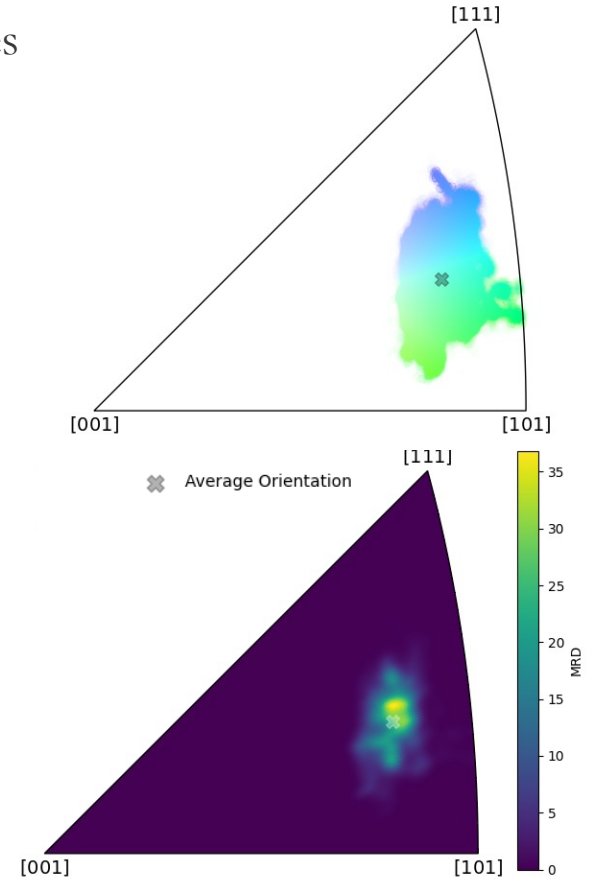

Complex 3D microstructures exhibit large orientation gradients

Spatial Representation

Orientation Representation (Cubochoric Space)

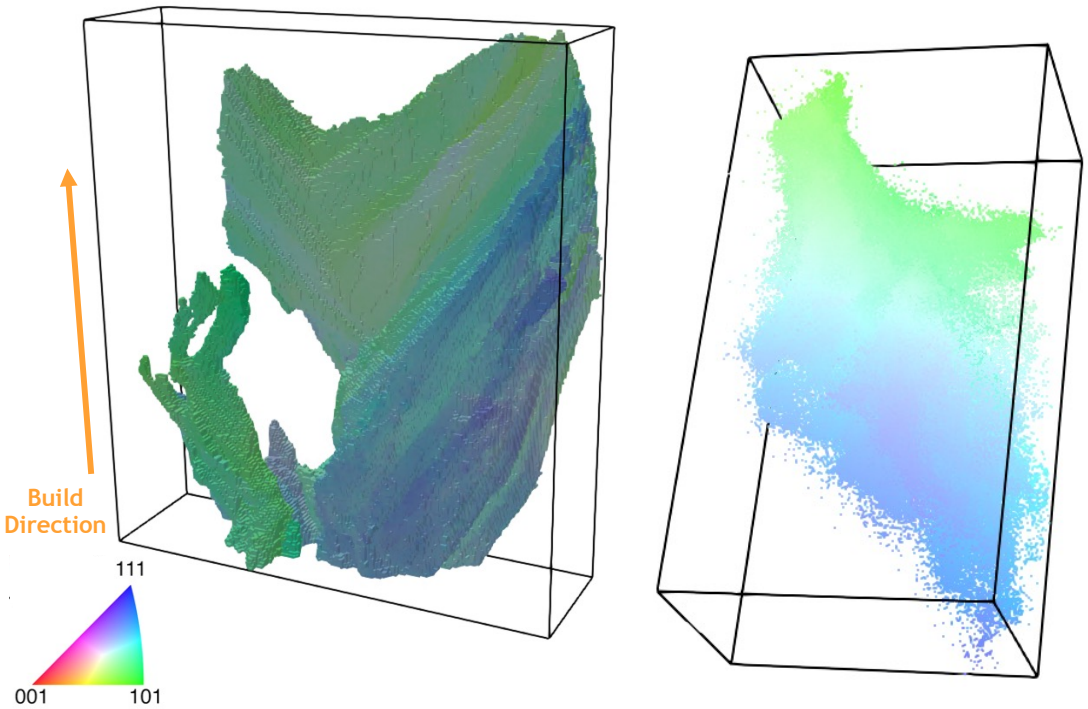

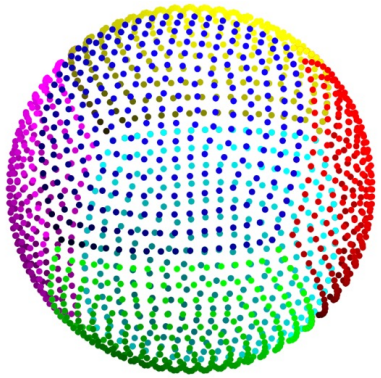

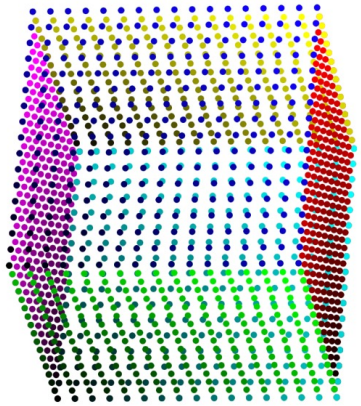

D Roşca. A Morawiec, and M De Graef, *Modelling and Simulation in Materials Science and Engineering*, 2014
S Singh and M D Graef, *Modelling and Simulation in Materials Science and Engineering*, 2016

Complex 3D microstructures exhibit large orientation gradients

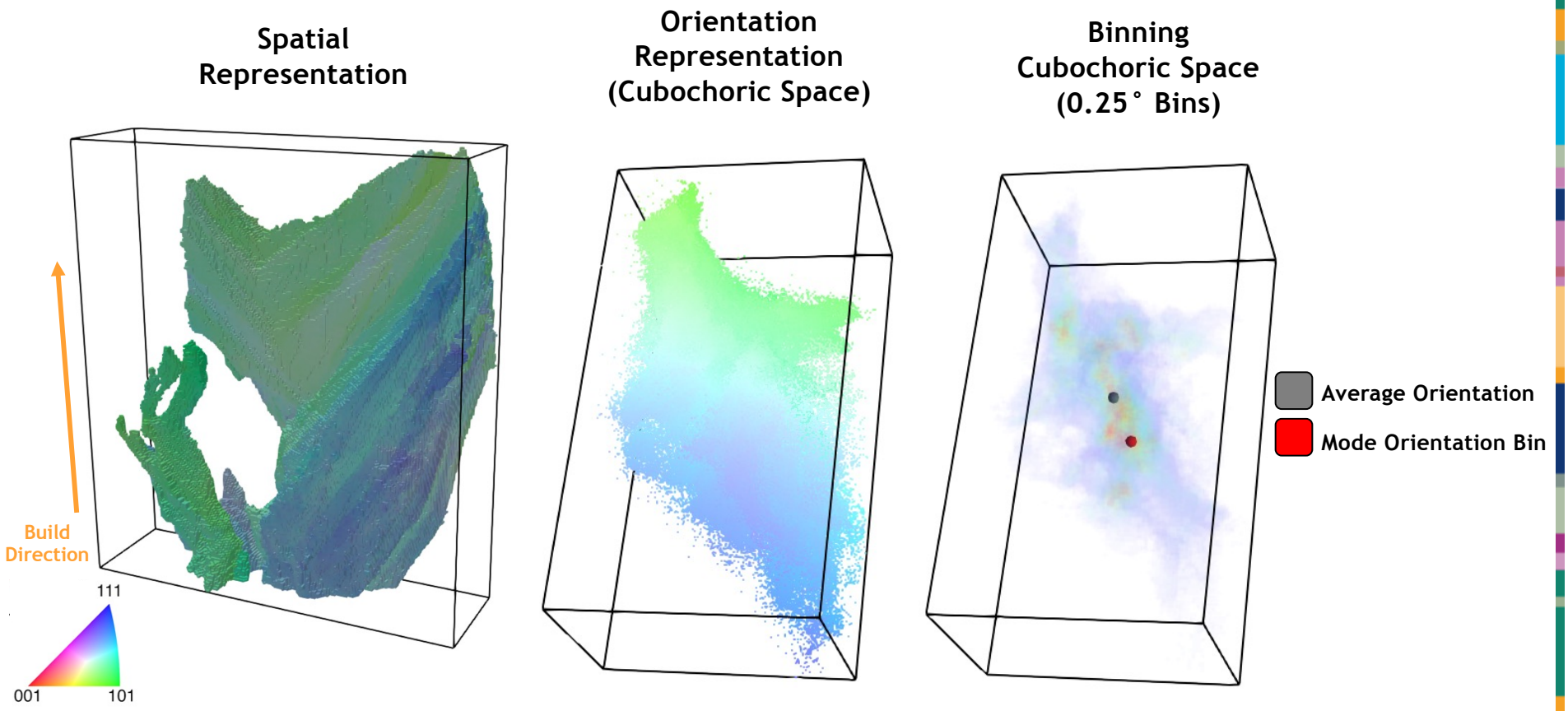

Complex 3D microstructures exhibit large orientation gradients

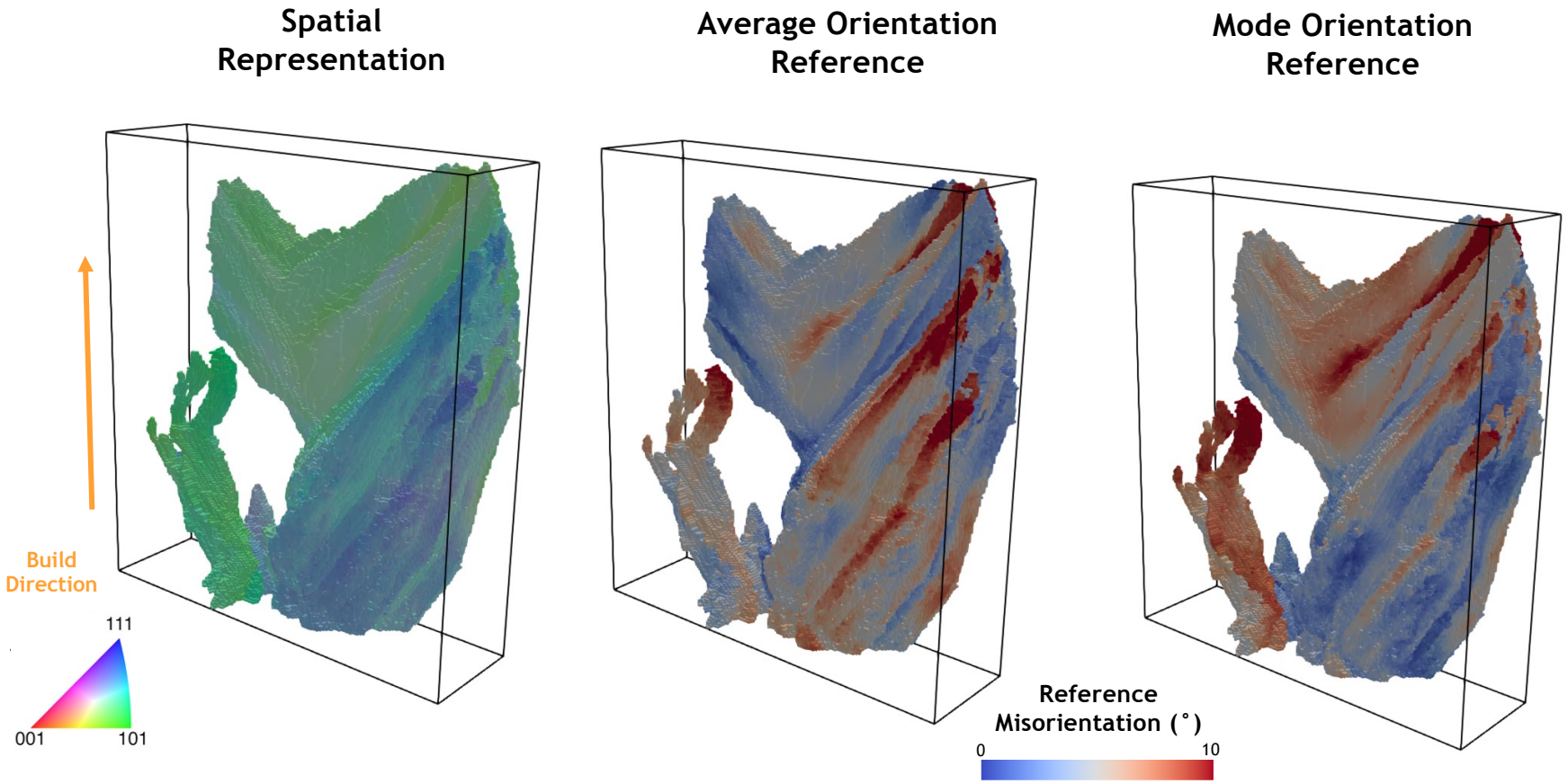

In situ tensile experiment with µCT and DCT

- Sample of Al 2219 processed with T6 heat treatment
  - Minimal texture
  - 55 µm average grain size
  - 0.3% porosity
  - 0.5% Al_2Cu Particles

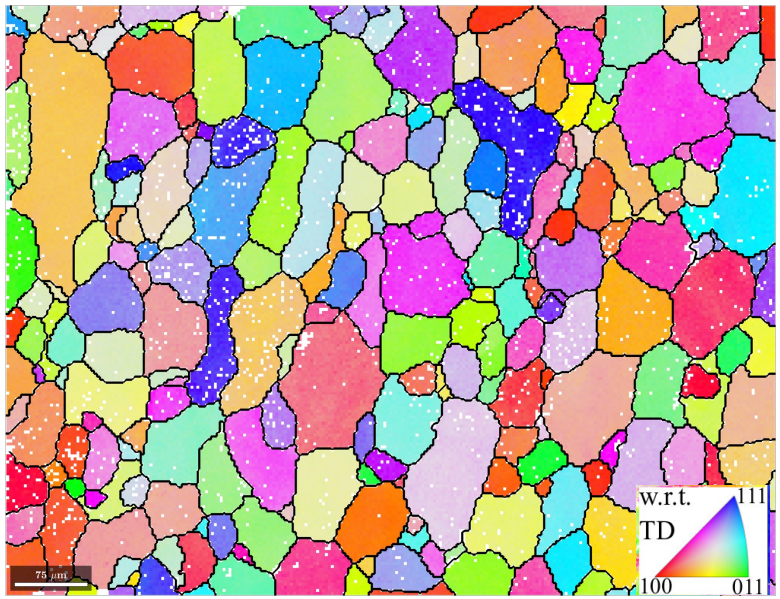

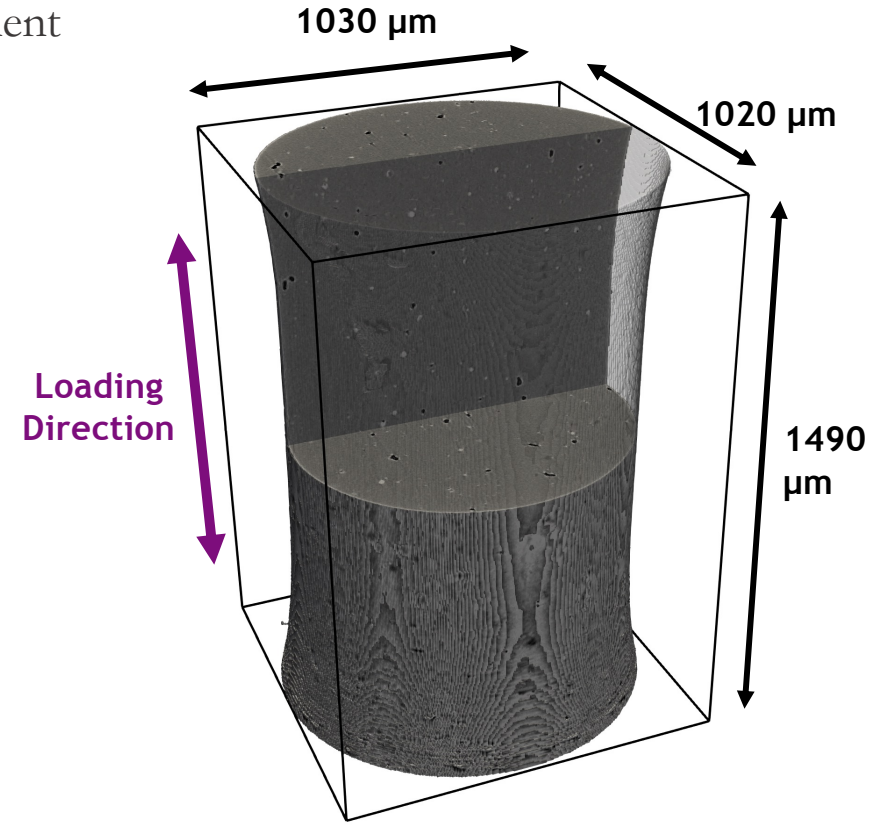

In situ tensile experiment with µCT and DCT

- Sample of Al 2219 processed with T6 heat treatment
  - Minimal texture
  - 55 µm average grain size
  - 0.3% porosity
  - 0.5% Al_2Cu Particles

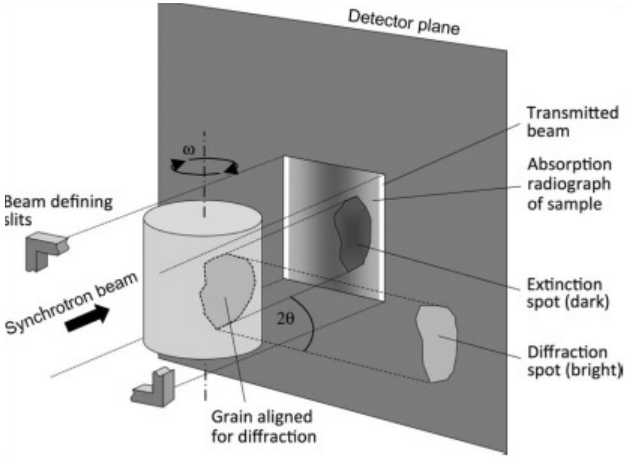

Image courtesy ESRF

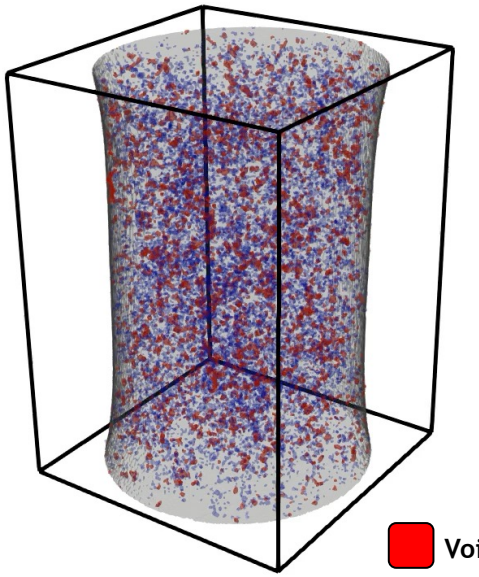

Voids

Precipitates

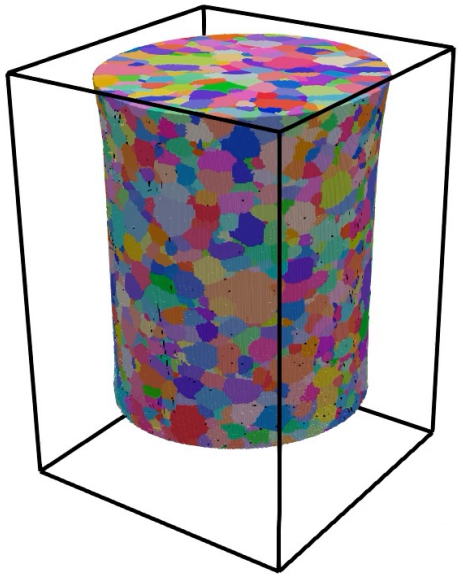

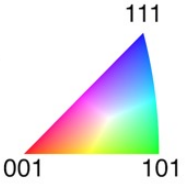

Reference Direction is Loading Direction (Z)

In situ tensile experiment with µCT and DCT

- 8 intermittent scans taken at fixed displacements until fracture

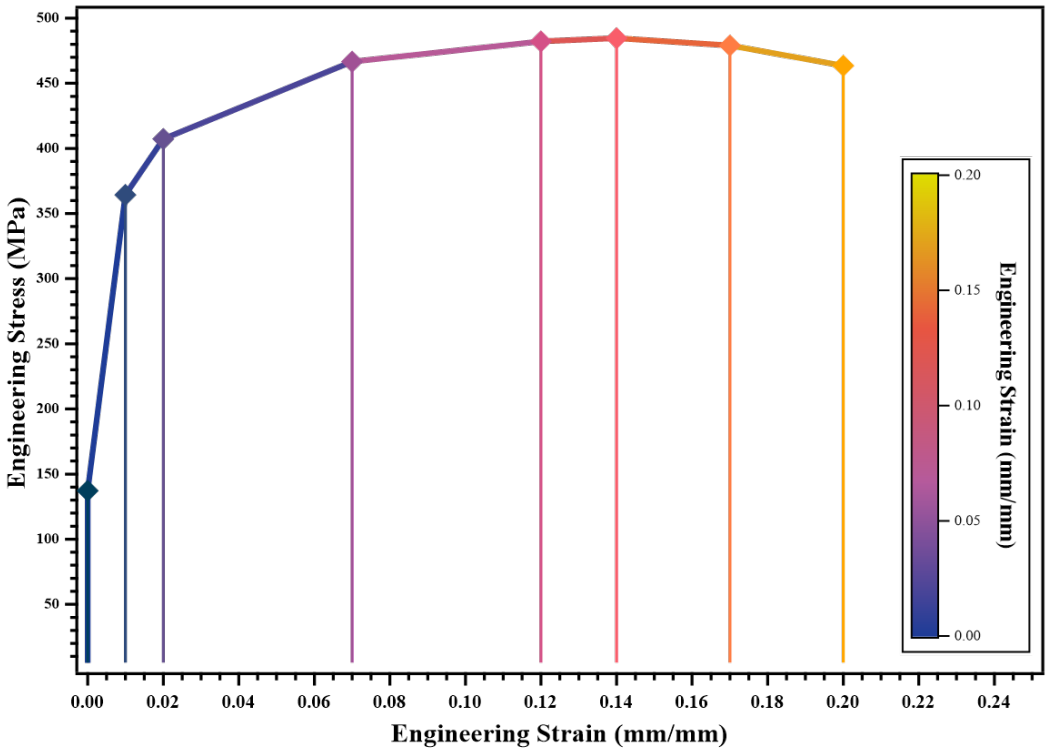

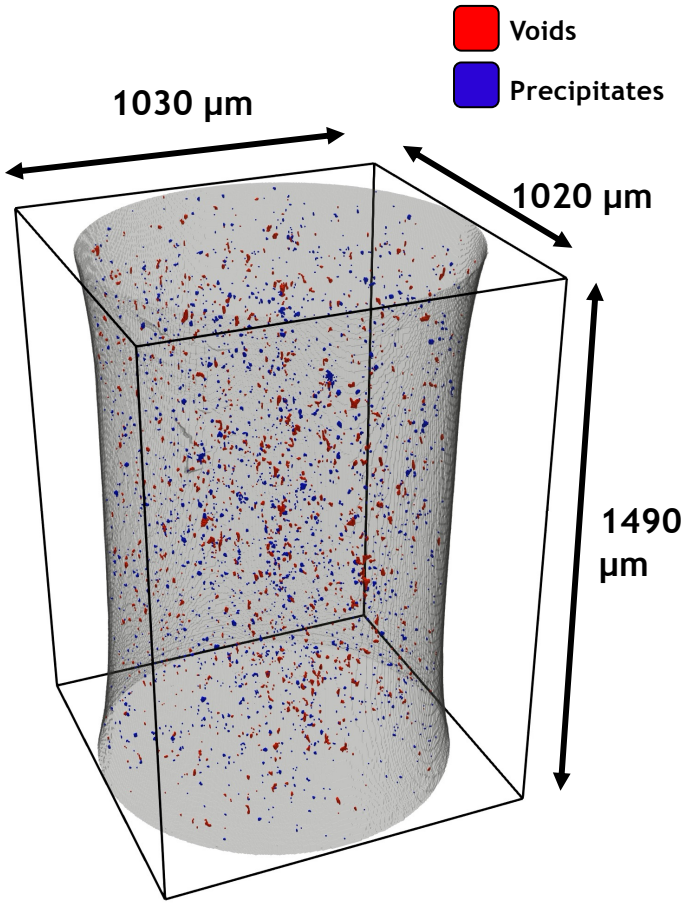

Ex situ analysis of fractured sample

- Understand deformation via orientation analysis
  - DCT cannot handle large deformations
- Utilized destructive serial sectioning in the SEM via TriBeam Tomography
- Ultimately want to fuse all data modalities into a single reference frame

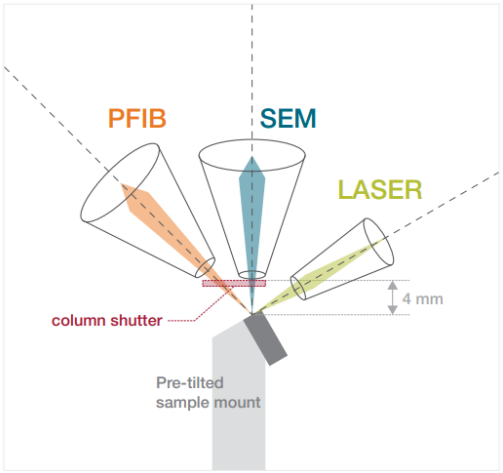

Image courtesy Thermo Fisher Scientific

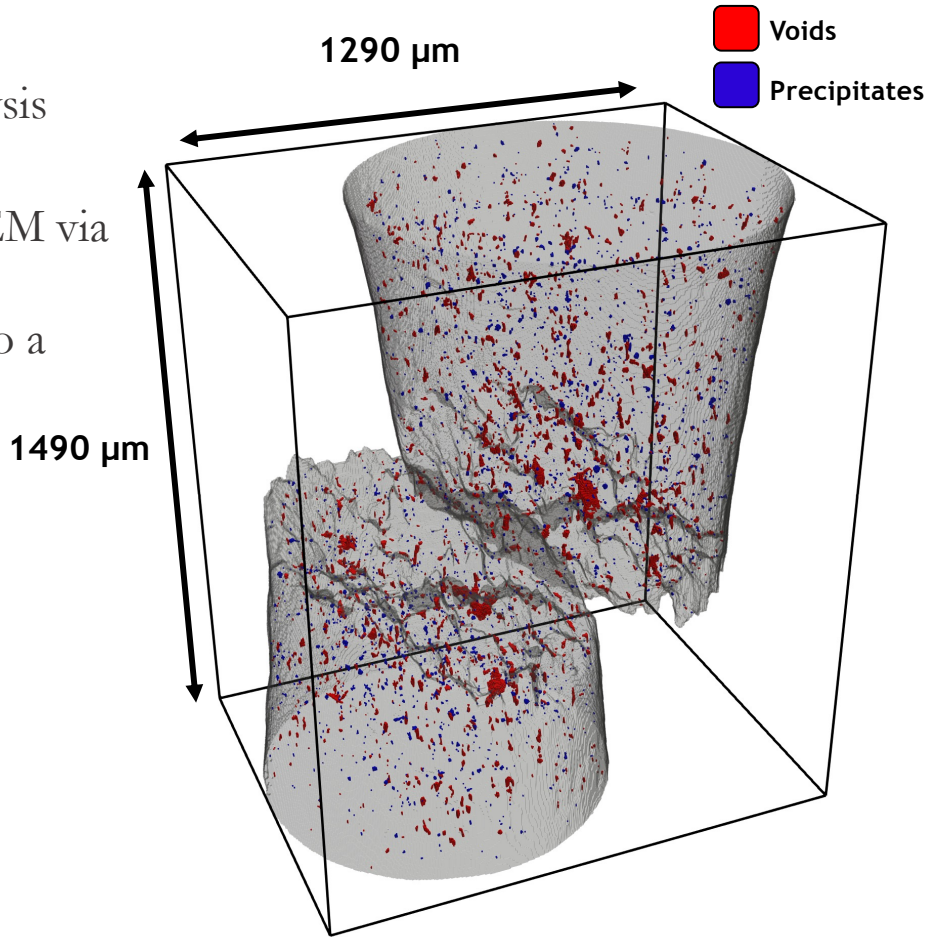

Backscatter Electron Image Flythrough

- Roughly 300 slices collected at a slice thickness of 2.0 μm
  - EBSD data also collected on each slice
  - Data collection is fully automated via in-house codebase using python interface with the SEM (autoscript package)
- Fracture surface shows mixture of transgranular and intergranular fracture
- Precipitates, voids, and cracks clearly visible in this imaging modality

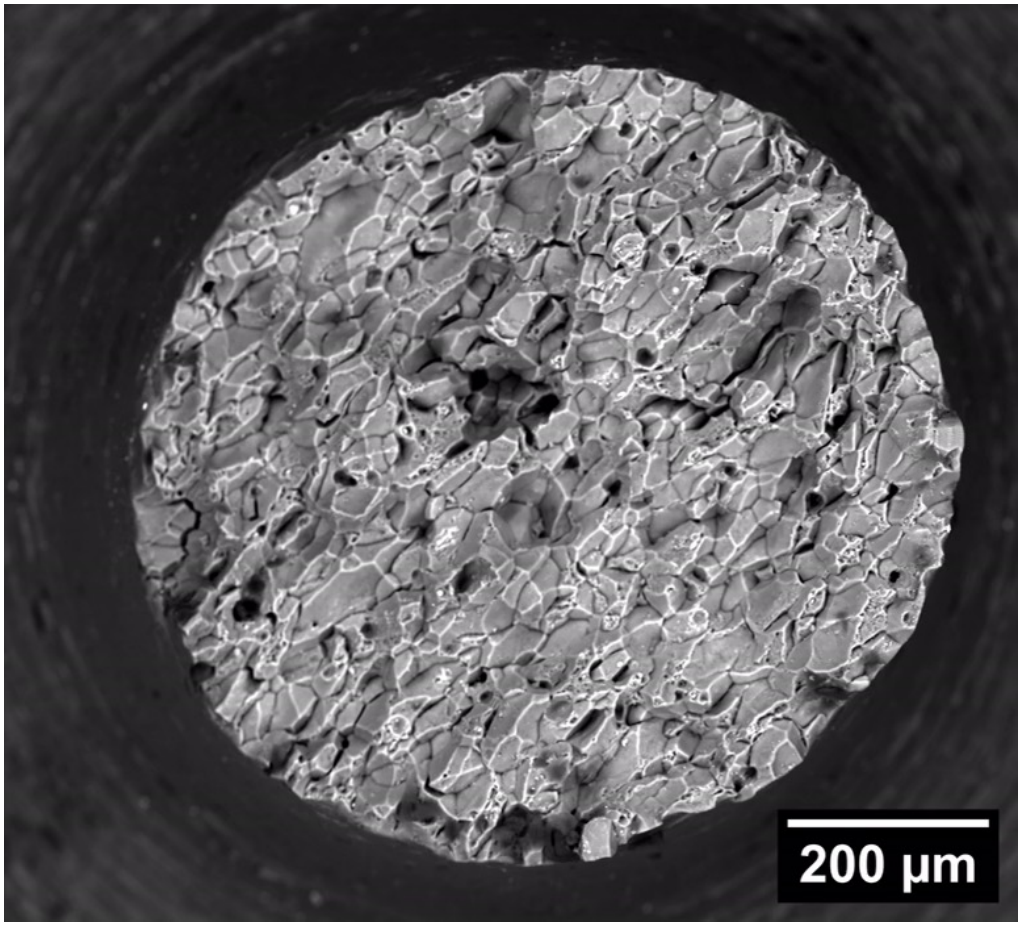

Fracture Surface Profile Comparison

- Serial-sectioning captures surface profile well, but is rotated in 3D relative to the CT data

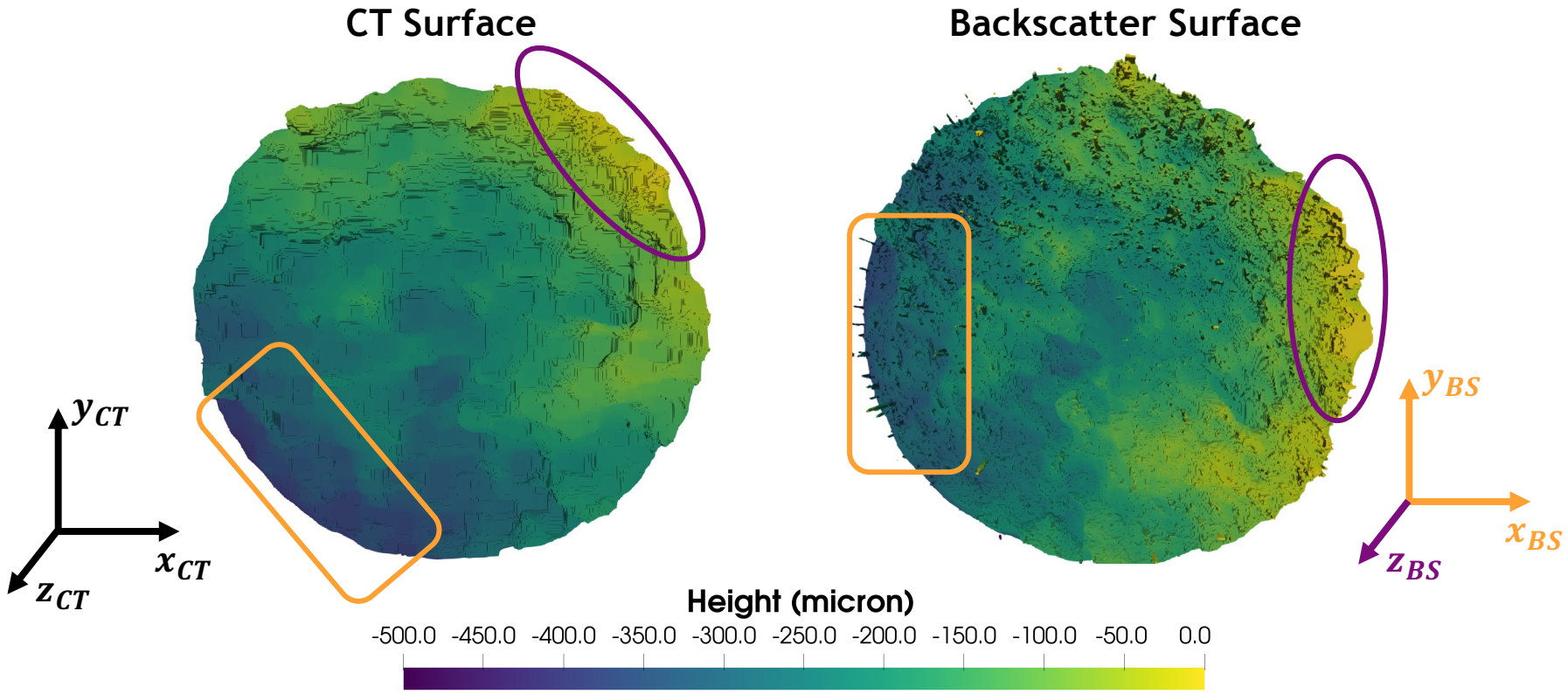

CT-Backscatter Data Fusion

- Following approach of Lenthe et al. (2015) for least-squares affine transformation using a series of control points:

$$[A] \leftarrow \begin{bmatrix} a_1^x & a_1^y & a_1^z & 1 \\ a_2^x & a_2^y & a_2^z & 1 \\ \vdots & \vdots & \vdots & \vdots \\ a_n^x & a_n^y & a_n^z & 1 \end{bmatrix}$$

$$[B] \leftarrow \begin{bmatrix} b_1^x & b_1^y & b_1^z & 1 \\ b_2^x & b_2^y & b_2^z & 1 \\ \vdots & \vdots & \vdots & \vdots \\ b_n^x & b_n^y & b_n^z & 1 \end{bmatrix}$$

$$[T] \leftarrow A^T B \left(B^T B\right)^{-1}$$

for all *voxels* in data set A **do**
  $x \leftarrow [centroid(voxel), 1]$
  $x' \leftarrow [T]^{-1} x$
  $v_b \leftarrow$ voxel nearest x'
  $voxel \leftarrow data(v_b)$
end for

WC Lenthe et al., *Journal of Applied Crystallography*, 2015

Backscatter Data

CT Data

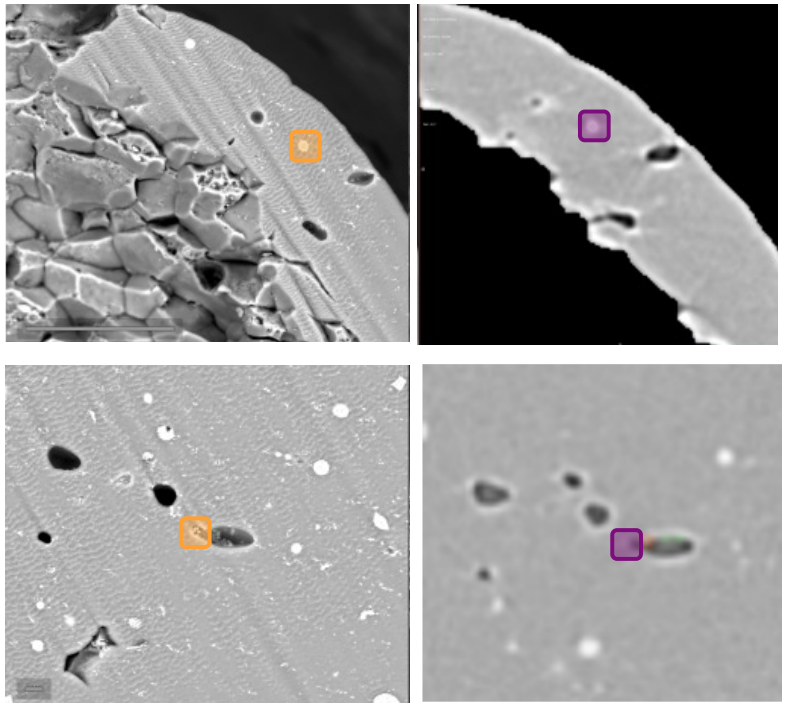

CT-Backscatter Data Fusion

- Mapping to new reference frame yields unified coordinate system

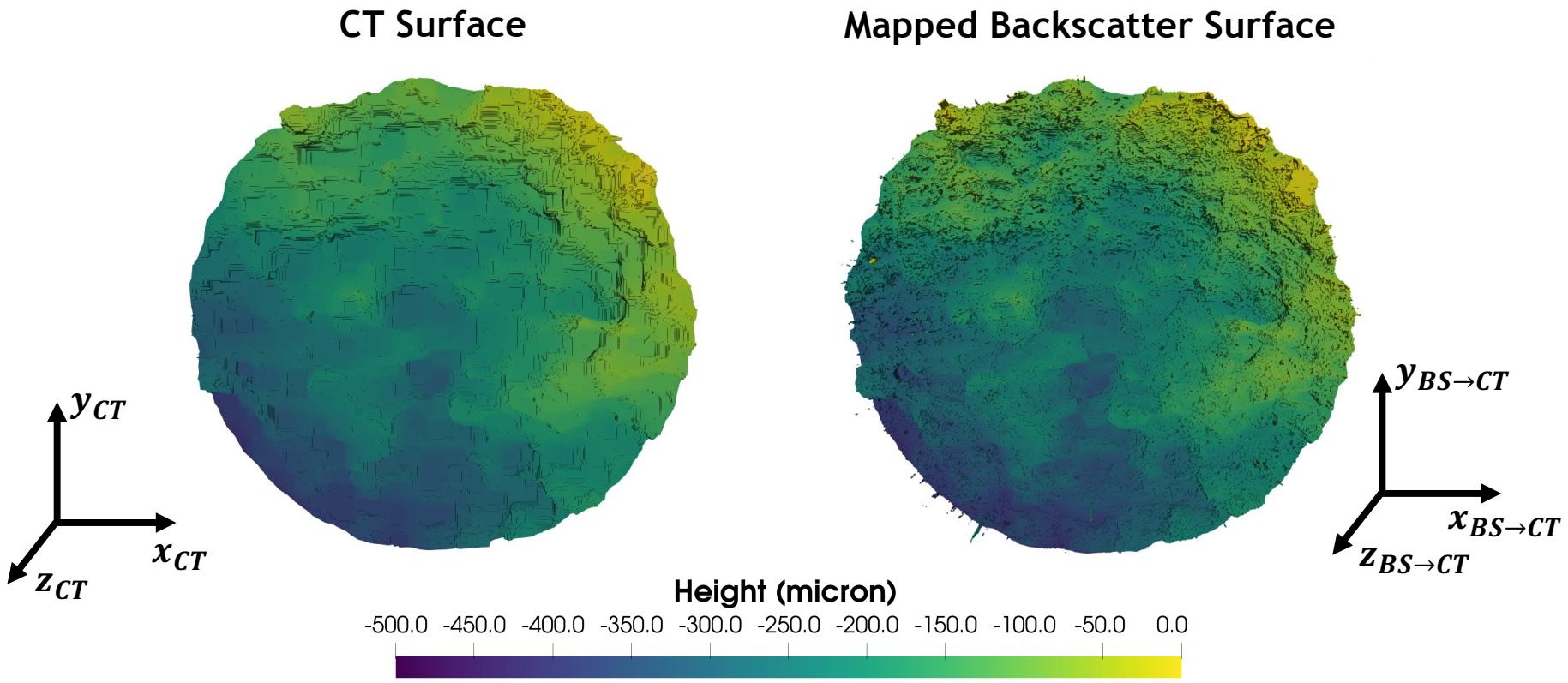

CT-Backscatter Data Fusion

- Mapping to new reference frame yields unified coordinate system

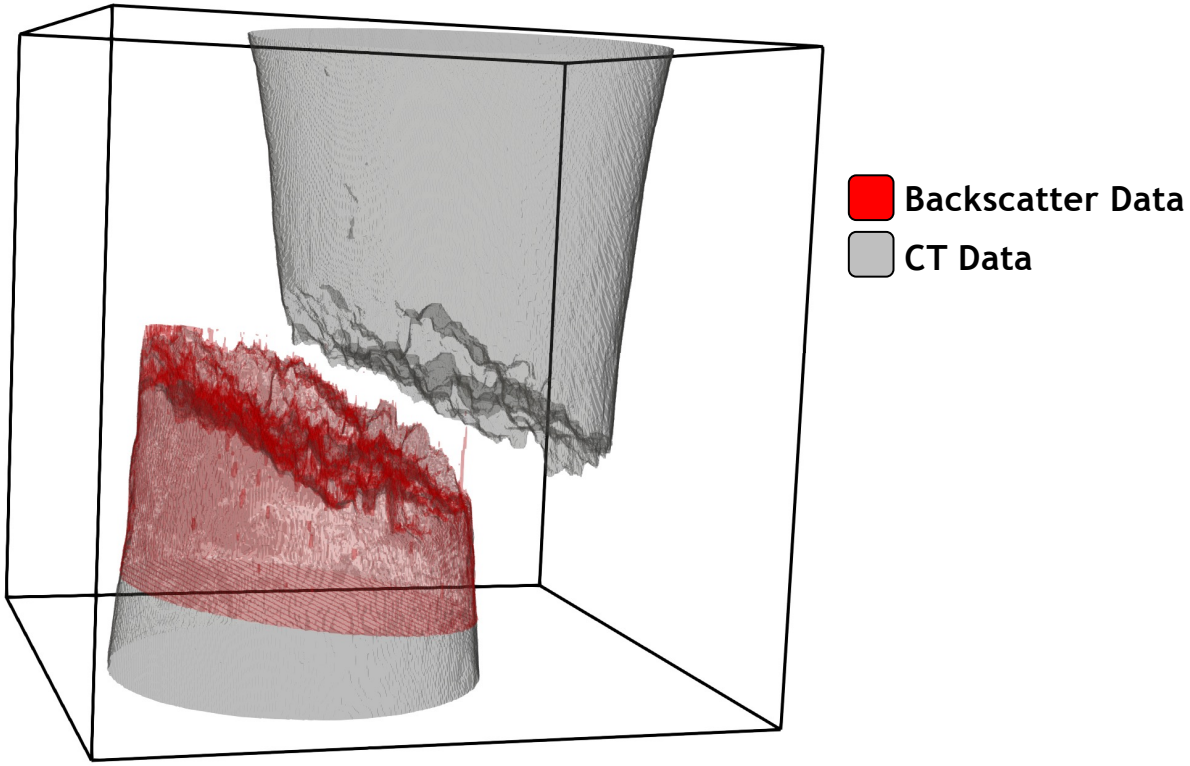

EBSD-Backscatter Data Fusion

- Distortions in EBSD are generally non-affine

Backscatter Image

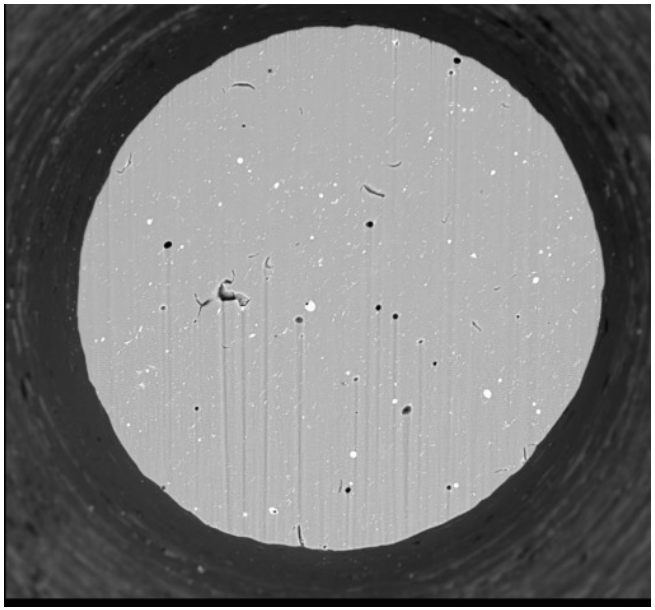

EBSD Image Quality

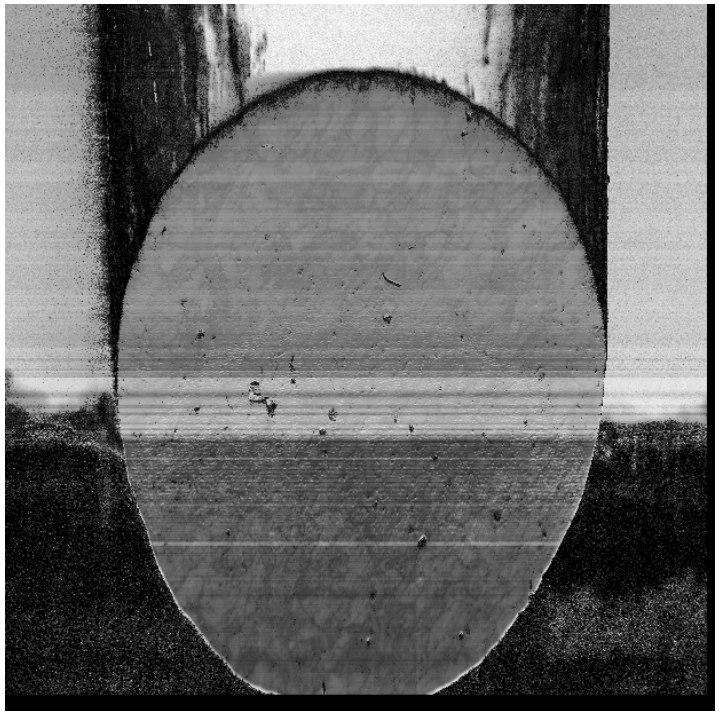

EBSD-Backscatter Data Fusion

- Thin-plate spline enables non-linear relation of reference frames using control points

Affine Portion **Bending Portion**

$$(X, Y, Z) = f(x, y, z) = a_1 + a_x x + a_y y + a_z z + \sum_{i=1}^{n} w_i U(|P_i - (x, y, z)|)$$

n = Control Points in distorted image (X_i, Y_i, Z_i) and reference image (x_i, y_i, z_i)

Backscatter Image (x, y, z)

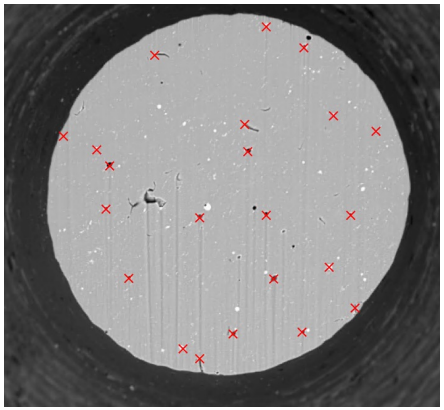

EBSD Image Quality (X, Y, Z)

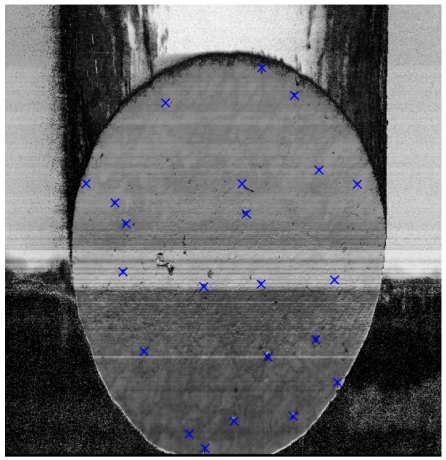

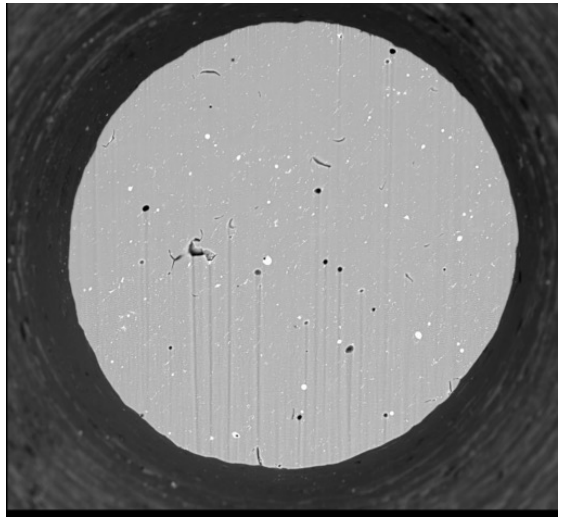

AT Polonsky et al., *Superalloys* (2020)

EBSD-Backscatter Data Fusion

- Thin-plate spline enables non-linear relation of reference frames using control points

Affine Portion **Bending Portion**

$$(X, Y, Z) = f(x, y, z) = a_1 + a_x x + a_y y + a_z z + \sum_{i=1}^{n} w_i U(|P_i - (x, y, z)|)$$

n = Control Points in distorted image (X_i, Y_i, Z_i) and reference image (x_i, y_i, z_i)

Backscatter Image (x, y, z)

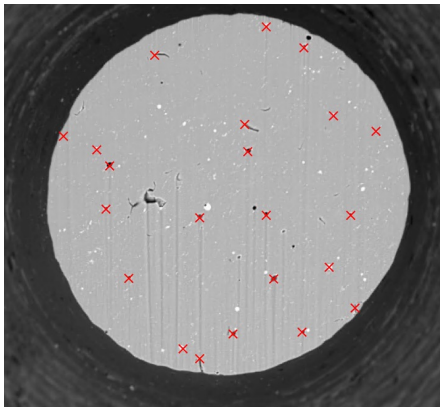

EBSD Image Quality (X, Y, Z)

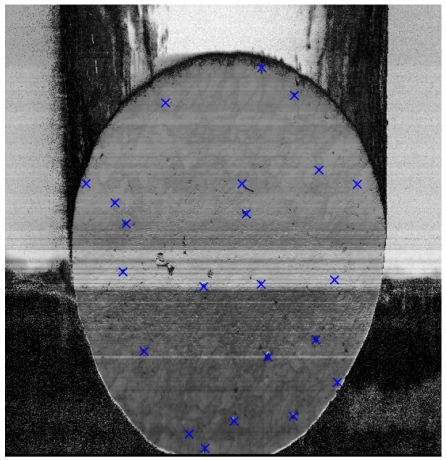

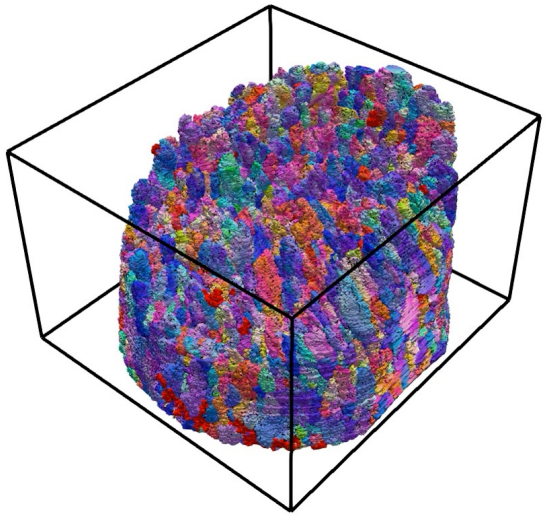

AT Polonsky et al., *Superalloys* (2020)

EBSD-Backscatter-CT Data Fusion

- Apply BS→CT transformation to distortion-corrected EBSD volume

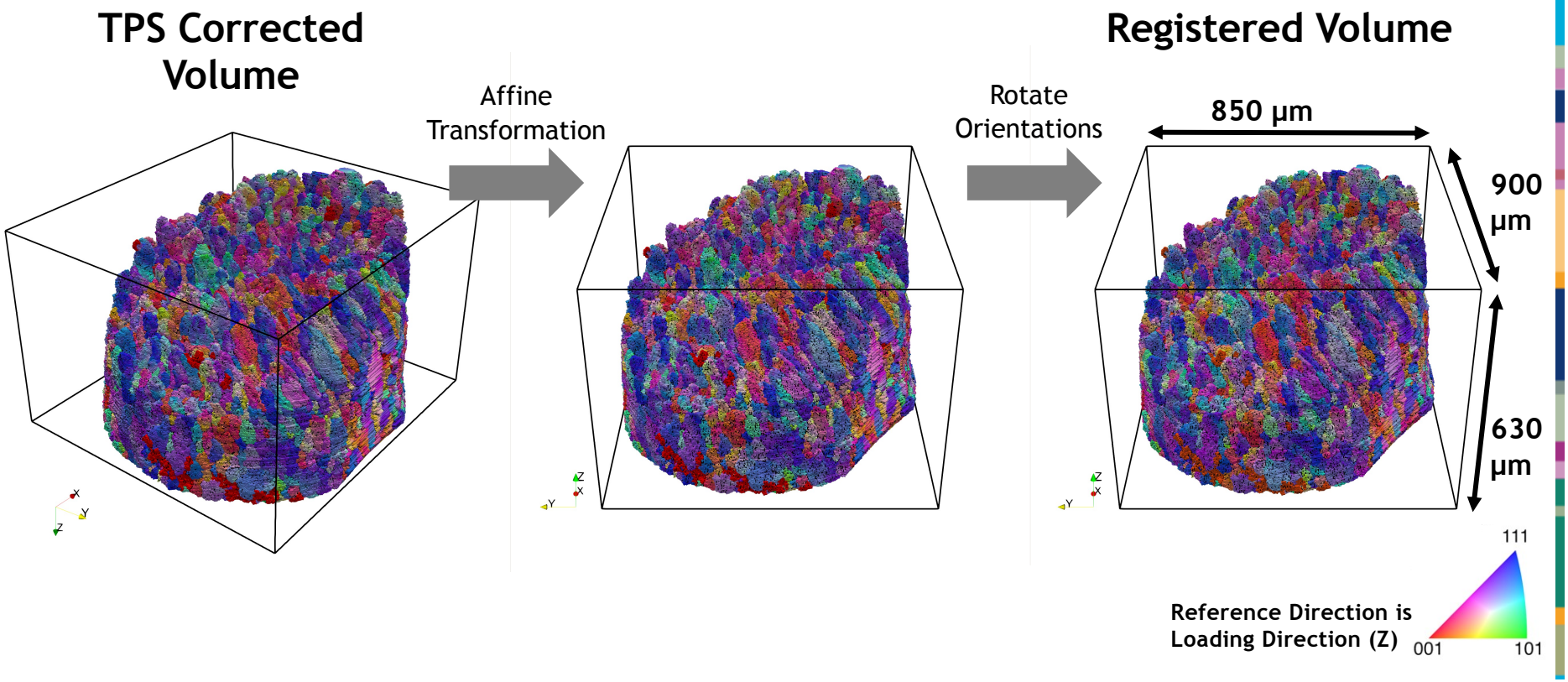

Intragrain misorientation distributions (mode reference)

- Linkage between distance from fracture surface and total misorientation accumulation at failure

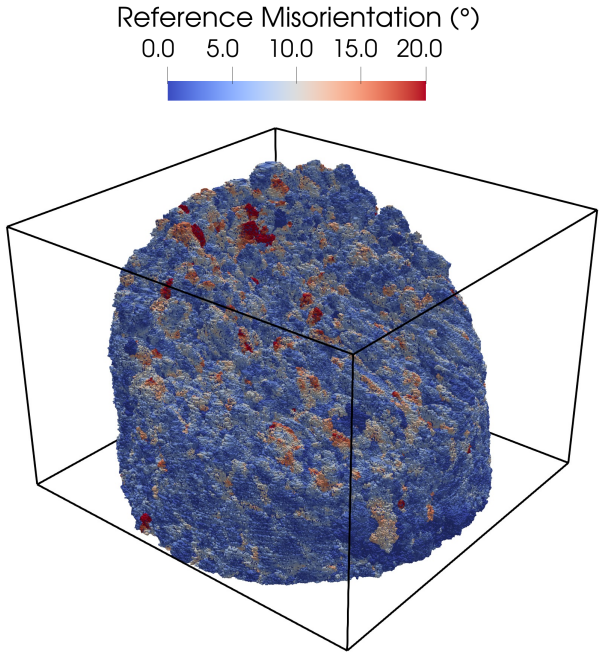

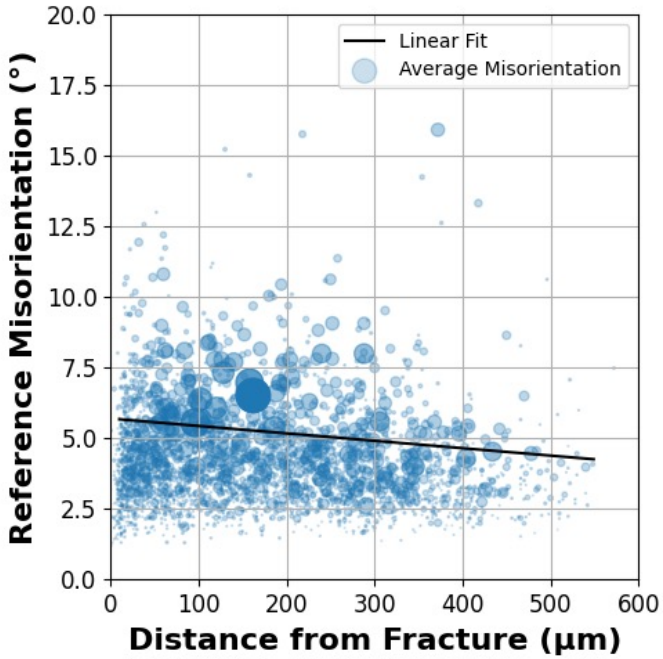

Clear changes in texture and morphology during deformation

- DCT Data (5 μm resolution)

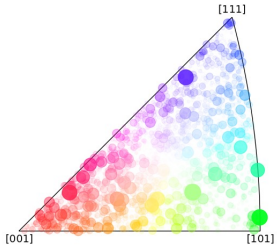

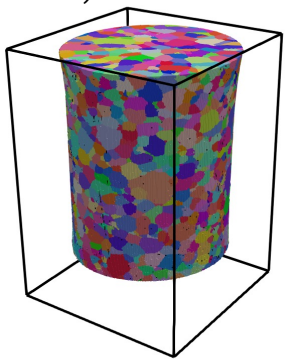

- EBSD Data (2 μm resolution)

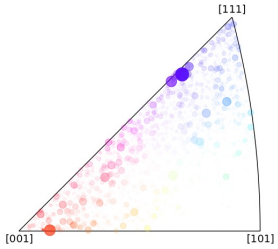

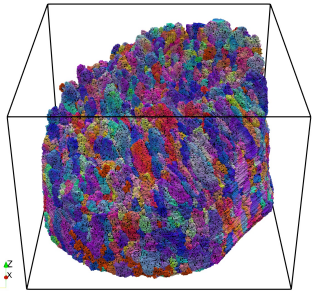

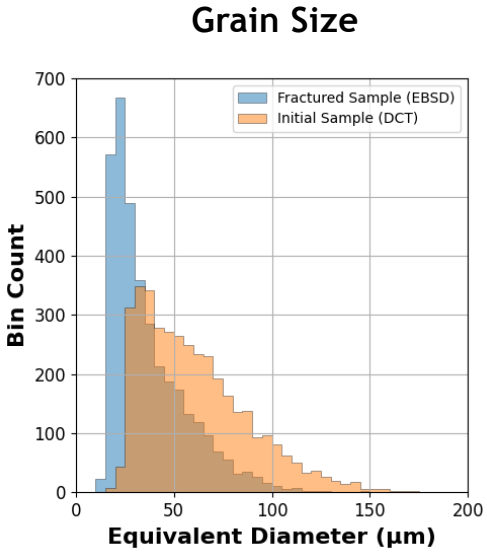

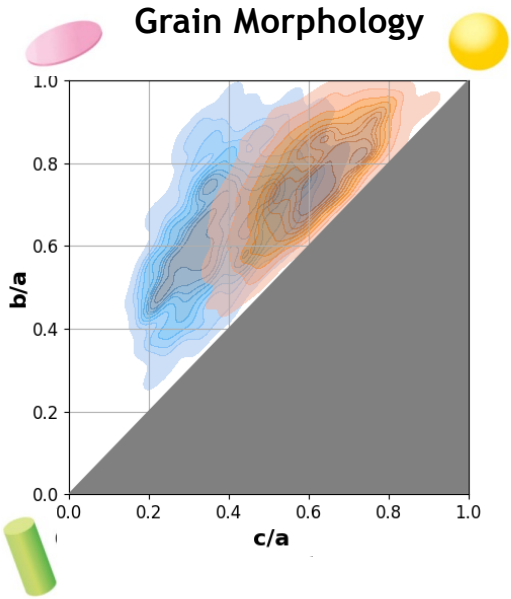

Crystal plasticity simulation initialized from DCT data

Sandia National Laboratories

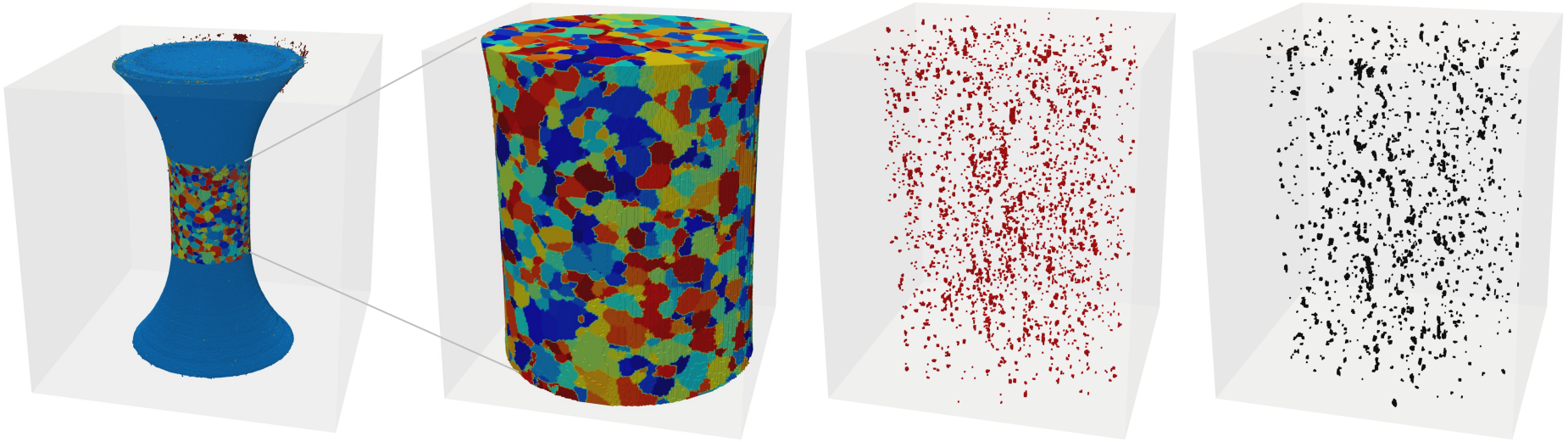

674x672x686
310,708,608 voxels
5um voxel size

209x206x245
10,548,230 voxels
3708 grains

Particle = 0.8865 %

Pores = 0.5055 %

CP Local Fields at 19% Strain

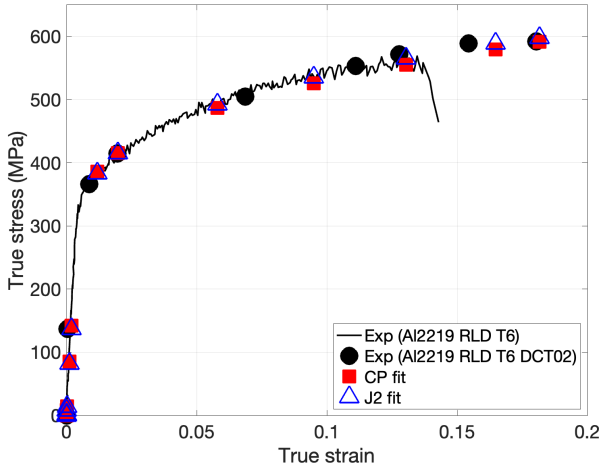

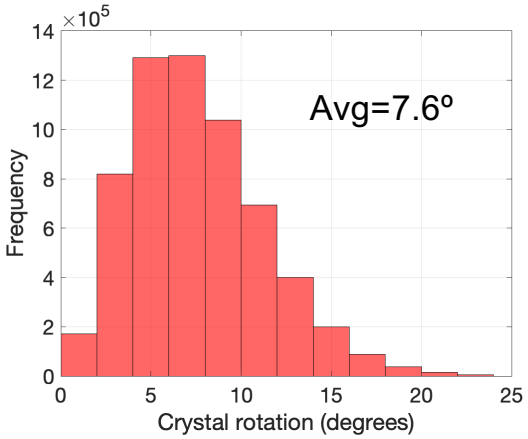

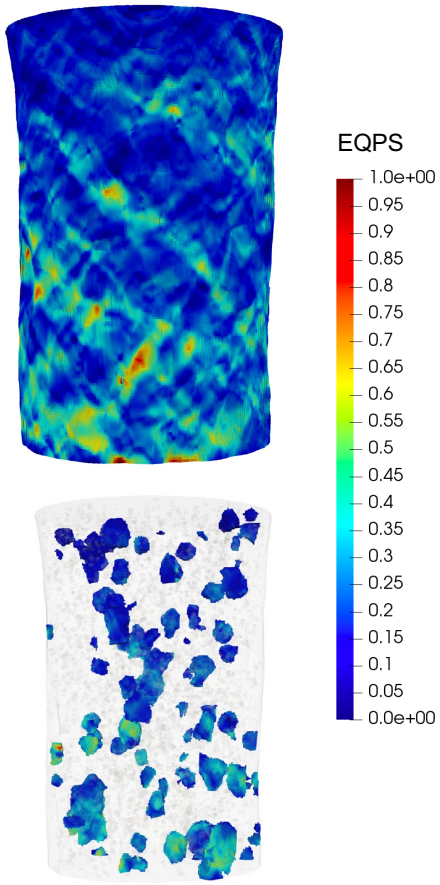

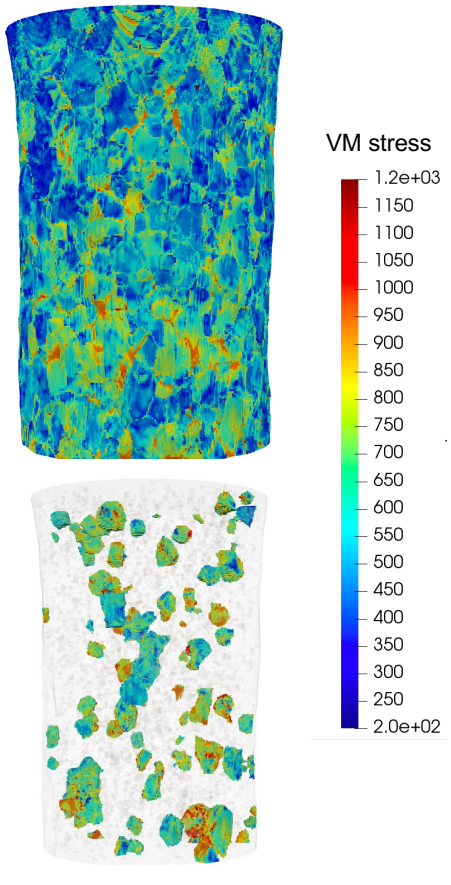

Grain rotation seen with CP explains change in texture

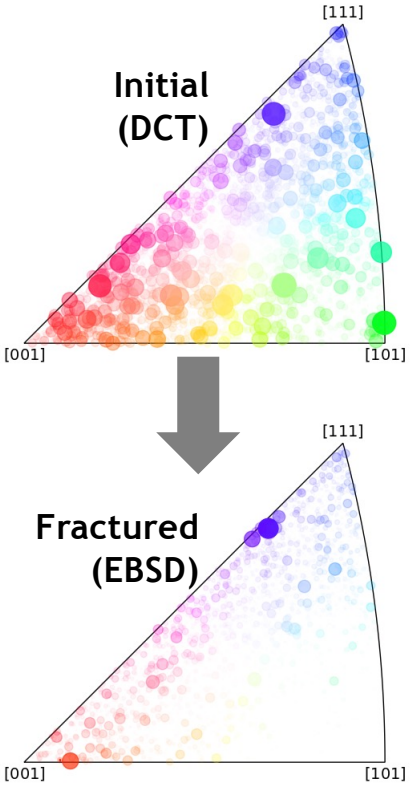

CP results from single grain:

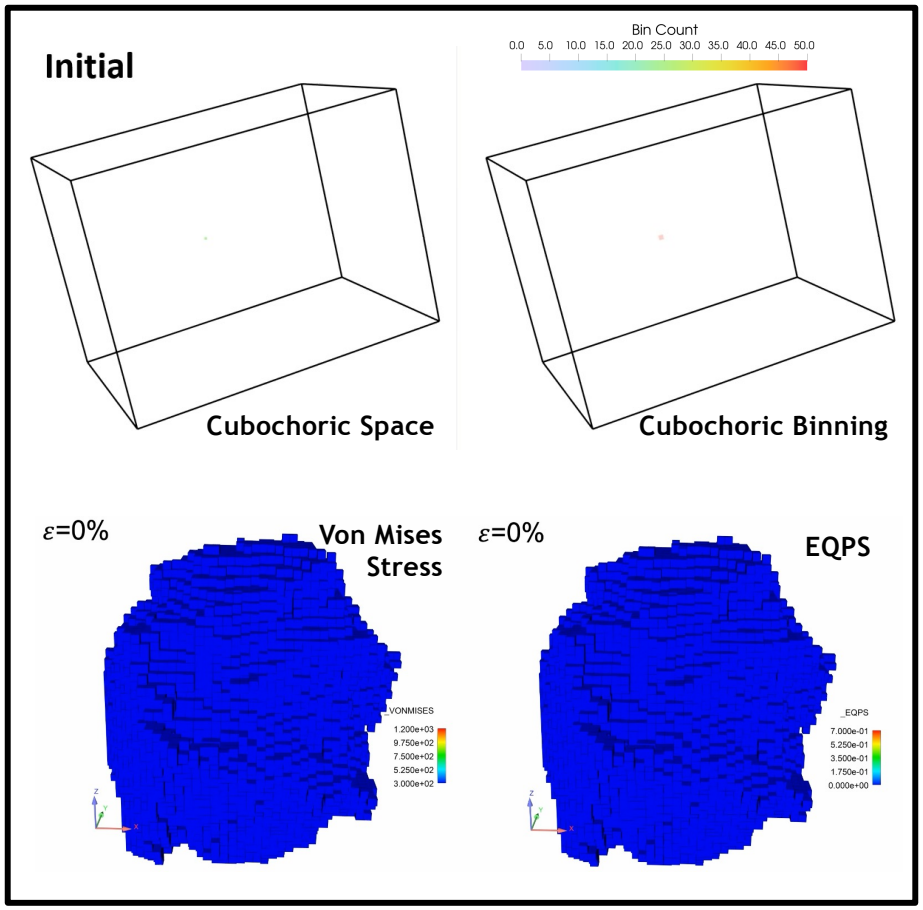

Grain rotation seen with CP explains change in texture

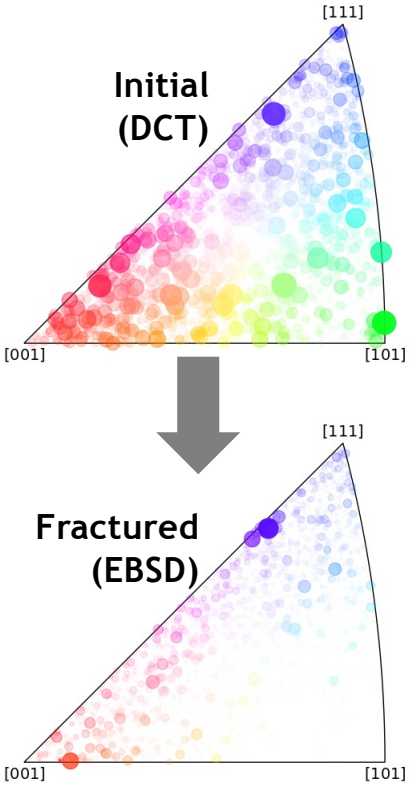

CP results from single grain:

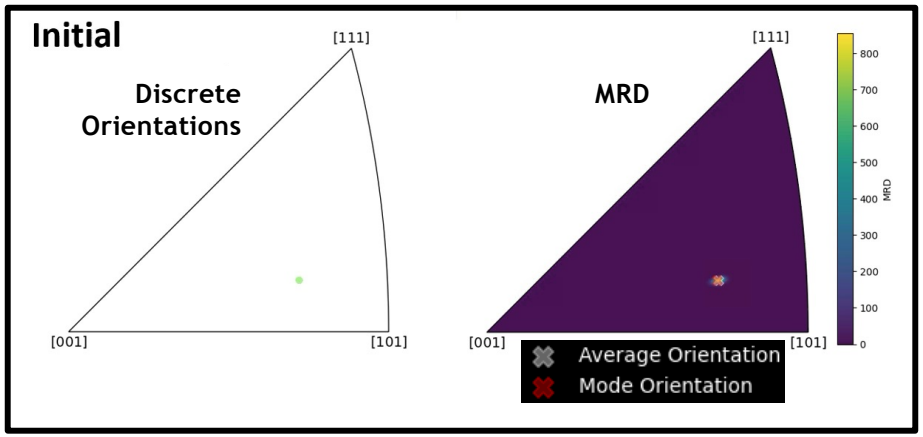

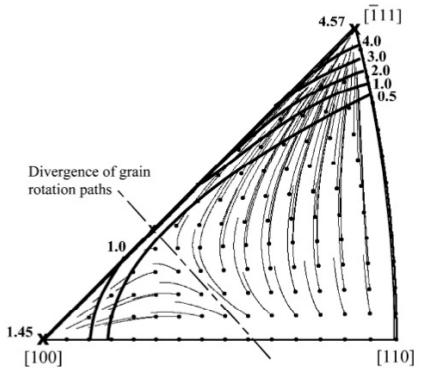

TE Buchheit, GW Wellman, CC Battaile, *International Journal of Plasticity*, 2005

Grains Pairs in undeformed DCT and fractured TriBeam data

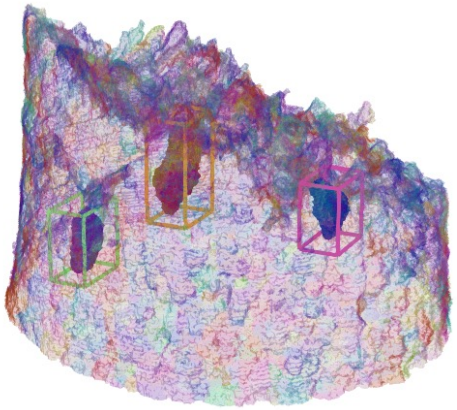

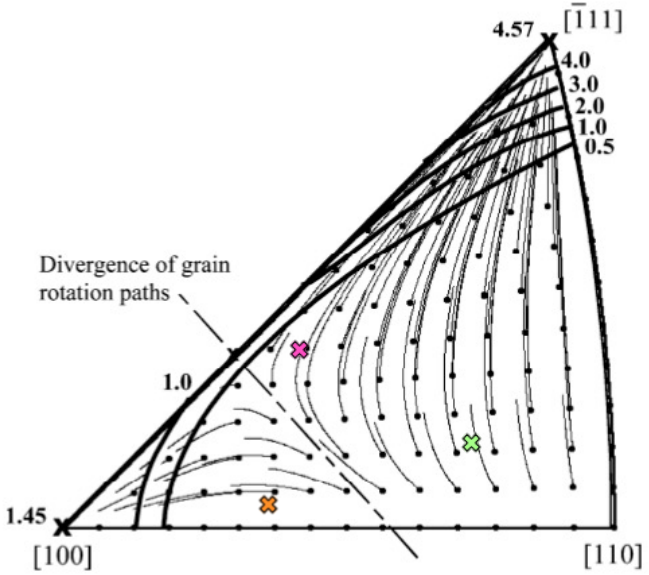

TE Buchheit, GW Wellman, CC Battaile, *International Journal of Plasticity*, 2005

Grains Pairs in undeformed DCT and fractured TriBeam data

Undeformed (DCT)

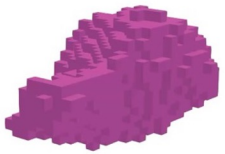

Fractured (TriBeam)

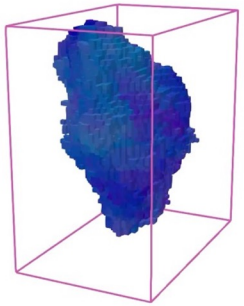

Experimental

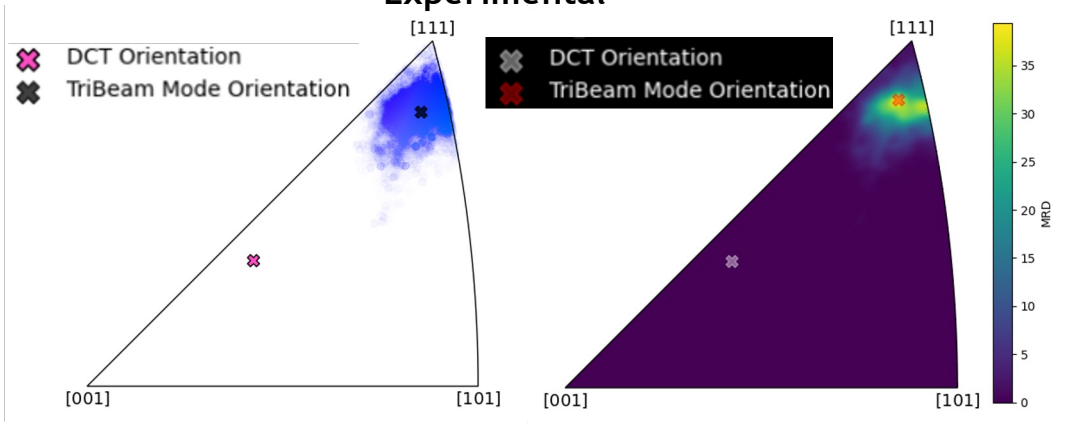

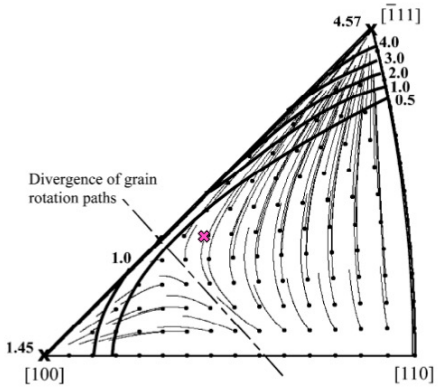

Modeling

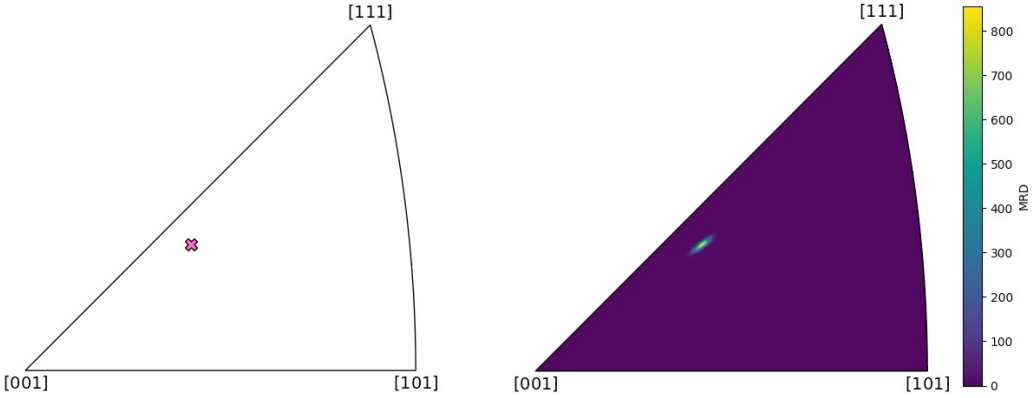

Grains Pairs in undeformed DCT and fractured TriBeam data

Undeformed (DCT)

Fractured (TriBeam)

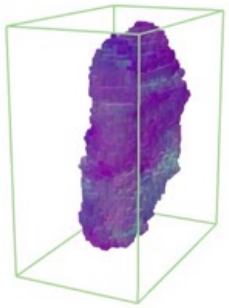

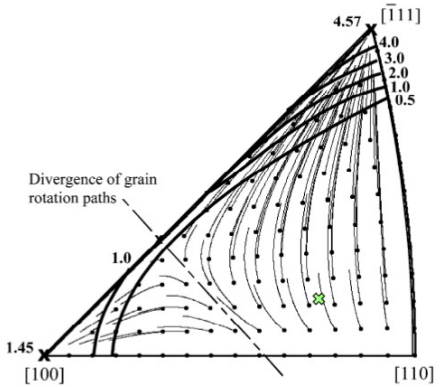

Experimental

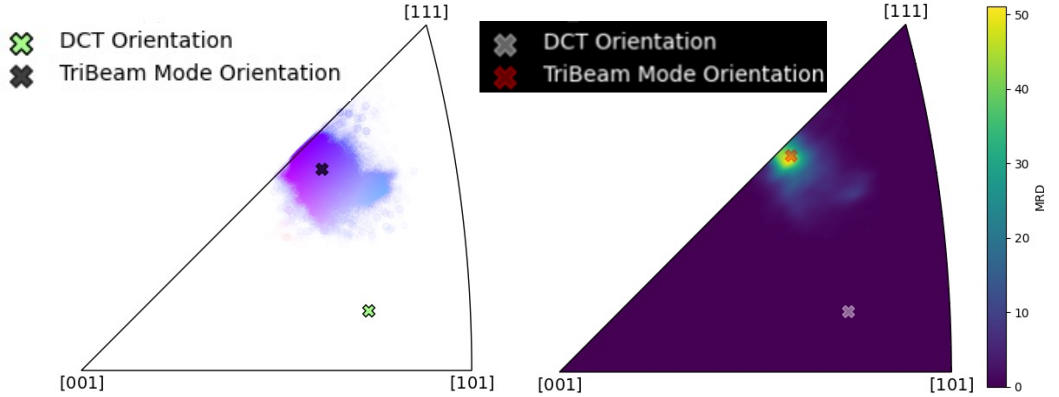

Modeling

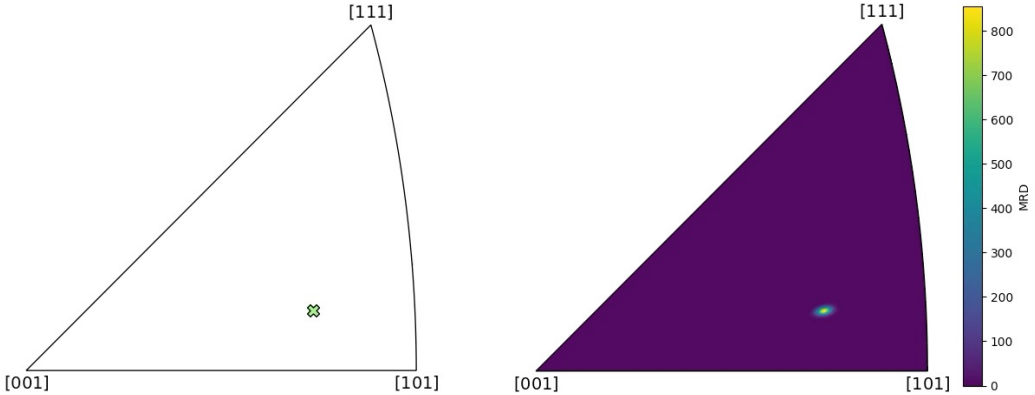

Grains Pairs in undeformed DCT and fractured TriBeam data

Undeformed (DCT)

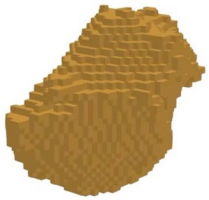

Fractured (TriBeam)

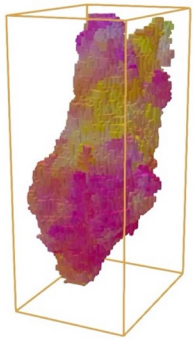

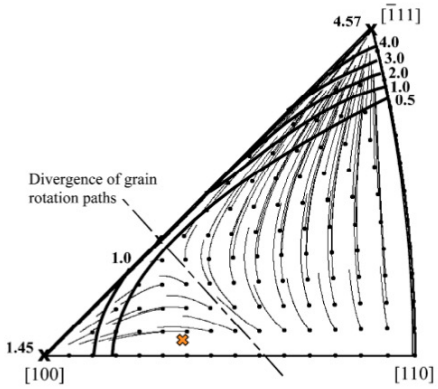

Experimental

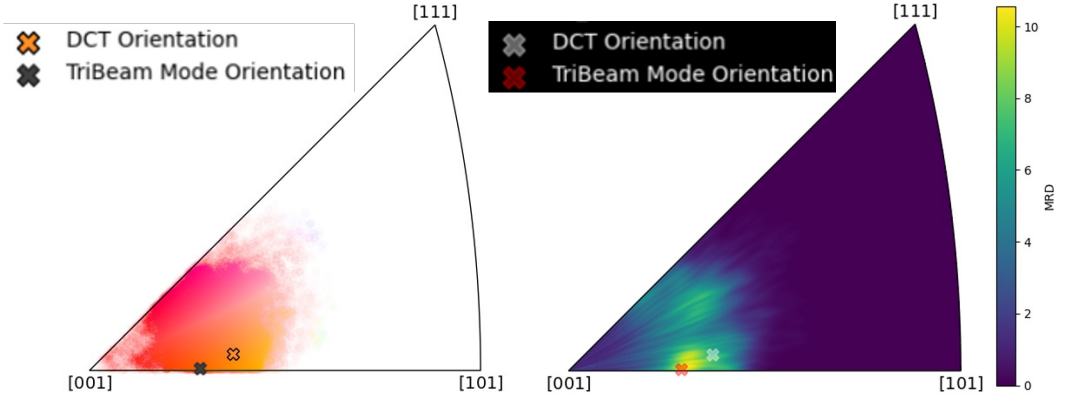

Modeling

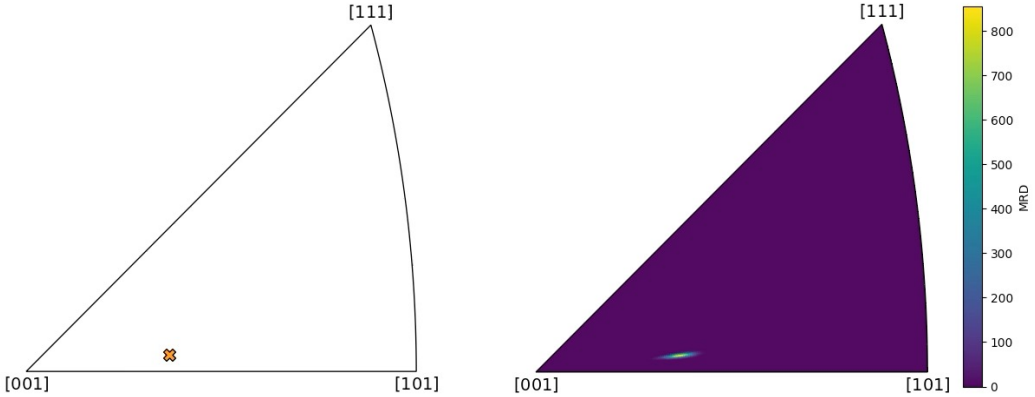

Conclusions

- Improvements in characterization approaches offers new opportunities for 3D EBSD to understand microstructure
- For complex microstructures with large orientation gradients, choice of reference orientation must be considered
- Data fusion with 3D EBSD is best approached as a combination of affine and non-affine transformations
- Ground truth EBSD data can be used to benchmark and improve high-fidelity modeling approaches